Comparing EMG Continuous Movement Decoding with Joints Unconstrained and Constrained

Lizhi Pan *Member, IEEE*, Zhongyi Ding, Jianmin Li* *Member, IEEE*

***Abstract*—Electromyography (EMG) signals have been employed for continuous movement decoding in recent years. However, several studies demonstrated that due to physiological factors, the EMG signals of amputees were poorer with respect to that of the able-bodied subjects. Our previous study demonstrated that the joint movements affected the performance of EMG pattern recognition. In this study, we aimed to investigate whether the movement of metacarpophalangeal (MCP) and wrist joints have effects on the performance of EMG continuous movement decoding. Six able-bodied subjects performed MCP and wrist flexion/extension simultaneously or independently with the MCP and wrist joints unconstrained (MWJU) and constrained (MWJC), while the EMG signals of the four forearm muscles were recorded. The musculoskeletal model was used to predict the joint angles from EMG signals. The performance of continuous movement decoding was quantified by the Pearson's correlation coefficient (r) and the normalized root mean square error (NRMSE) between the measured and predicted joint angles. The results showed that the MWJC significantly reduced the prediction performance of continuous movement for all subjects when compared to the MWJU. The average r values of the wrist and MCP flexion/extension decreased from 0.89 to 0.82 and 0.86 to 0.52, respectively. The average NRMSE values of the wrist and MCP flexion/extension increased from 0.18 to 0.21 and 0.22 to 0.31, respectively. The results demonstrated that the movements of the MCP and the wrist joints have a significant effect on the continuous movement decoding. Our study revealed a potential factor inducing the poor performance of continuous movement decoding in amputees.**

***Index Terms*—Electromyography; continuous movement decoding; musculoskeletal model; comparison.**

I. Introduction

ELECTROMYOGRAPHY (EMG) are electrical signals accompanying muscle contractions. It is an important approach for the non-invasive detection of muscle activity from the skin surface [1]–[3]. Surface EMG (sEMG) signals are superpositions of muscle potentials that act as a substitute for the neural signals generated by the central nervous system [4]. Since sEMG signals contain rich physiological information, they are often used to decipher movement intentions [3].

Pattern recognition has been adopted to identify intended motions from EMG signals for more than 30 years [5]. Bellingegni et al. compared four different classifiers, such as nonlinear Logistic regression, multi-layer perceptron, support vector machine, and linear discriminant analysis, to evaluate the performance and computational effort of the algorithm [6]. The classification accuracy (CA) of EMG pattern recognition for able-bodied individuals attained $> 95\%$, while the CA of pattern recognition for amputees was less than 80% [7]–[10]. The CA of EMG pattern recognition of amputees is affected by several physiological factors, such as muscle atrophy of the residual limb [11] and the remaining length of the residual limb [12]. Our previous studies investigated the effect of hand and wrist movement on EMG classification performance [13]. The results demonstrated that the CA without joint movements decreased by 10% when compared to that with joint movements [14]. The studies indicated that no joint movement was a factor that caused the poor performance of EMG pattern recognition for amputees. However, the EMG pattern recognition only realized the discrete motion control of the prosthesis, which was different from the natural and smooth movement of humans. Users may prefer continuous and intuitive control [15].

To study continuous movement decoding from EMG signals, a variety of methods have been employed, such as artificial neural networks (ANN), linear regression (LR), nonlinear regression (NLR), non-negative matrix factorization (NMF), and state-space models (SSM) [16], [17]. Koike et al. achieved the continuous prediction of elbow and shoulder joint torques through a modular artificial neural network [18]. Ngeo et al. achieved estimation of continuous movement of finger joints using a fast feedforward ANN and a nonparametric Gaussian process (GP) regressor [19]. A hierarchical projection regression algorithm to estimate the continuous movement angles of the elbow joint online [20]. Domenico et al. developed Hannes prosthesis control based on a regression machine learning algorithm [21]. Ameri et al. achieved the application of a support vector machine (SVM)-based multi-degree-of-freedom (DOFs) real-time synchronous proportional EMG control scheme [22]. A switching regime model for EMG-based robotic arm control was proposed [23]. Pan et al. proposed a switching regime including one linear discriminant analysis (LDA) classifier

Manuscript received: May, 9, 2022; Revised June, 1, 2022; Accepted July, 4, 2022.

This paper was recommended for publication by Editor P. Valdastri upon evaluation of the Associate Editor and Reviewers' comments.

This work was supported in part by National Natural Science Foundation of China (Grant No. 52005364, 52122501). Asterisk indicates the corresponding author.

Lizhi Pan, Zhongyi Ding, and Jianmin Li* are with the key Laboratory of Mechanism Theory and Equipment Design of Ministry of Education, School of Mechanical Engineering, Tianjin University, Tianjin 300350, China. (Email: melzpan@tju.edu.cn; zyding_@tju.edu.cn; mjli@tju.edu.cn)

Digital Object Identifier (DOI): see top of this page.

and fourteen SSM for continuous decoding of finger joint angles [24]. However, all of these methods were based on the data-driven algorithms that used the numerical mapping between EMG signals and joint angles. Recently, several research groups investigated the feasibility of developing an EMG continuous movement decoder based on a musculoskeletal model [25], [26]. Compared to the data-driven approach, the model-based approaches had more physics significance because they took into account the physiological structure of the human body. A 2-DOFs musculoskeletal model was proposed to predict metacarpophalangeal (MCP) and wrist flexion/extension movements [27], [28]. A musculoskeletal model of the upper extremity was developed for using in the development of neuroprosthetic systems [29]. A biomimetic interface was proposed to synthesize the musculoskeletal function of an individual's phantom limb as controlled by neural surrogates [30]. Durandau et al. used a musculoskeletal model to calculate the forces of 13 lower-limb tendon units and estimate the moments of three DOFs in real-time. This framework can greatly reduce the evaluation delay in current clinical biomechanics and open up new ways to develop rapid and personalized treatment [31].

In this study, we aimed to study whether the movement of the MCP and wrist joints have effects on the performance of continuous movement decoding. Six able-bodied subjects were tested with two scenarios: MCP and Wrist Joints Unconstrained (MWJU) and Constrained (MWJC). The EMG signals and joint angles were recorded simultaneously. Since the joint angles cannot be collected under the condition of MWJC, the mirrored bilateral training was adopted to collect the intended joint angles. Pan et al. demonstrated that the musculoskeletal model could estimate joint movement more accurately than either LR or ANN [27]. Therefore, the EMG-driven musculoskeletal model was employed to predict the joint angles of the subjects during the single-DOF and simultaneous two-DOFs movements in the two scenarios. Then, the Pearson's correlation coefficient (r) and the normalized root mean square error (NRMSE) between the predicted and measured joint angles were calculated to quantify the performance of continuous movement decoding. We compared the performance of continuous movement decoding in these two scenarios.

II. Methods

A. Subjects

The study recruited and tested 6 able-bodied (Sub1 - Sub6) subjects (6 males, aged from 22 to 26 years, height: 1.75 m ± 0.1 m, weight: 60.0 kg ± 10.0 kg, all right-handed). All subjects had no known neuromuscular disorders. Informed consent forms were signed and given by the subjects. The testing procedure was approved by the Ethics Committee of Tianjin University (Approval #: TJUE-2021-114, Approval date: 05/23/2021) and complied with the latest version of the Declaration of Helsinki.

B. Experiments and Data Acquisition

Two different experimental scenarios were tested in this study: 1. MCP and Wrist Joints Unconstrained (MWJU); 2. MCP and Wrist Joints Constrained (MWJC). 1) MWJU: as shown in Fig. 1a, the subjects were instructed to sit on a chair with the elbow at 90°, the arm and fingers were in a natural state to perform the following 5 different types of movements: a) wrist flexion/extension only, rhythm; b) MCP flexion/extension only, rhythm; c) wrist flexion/extension only, random; d) MCP flexion/extension only, random; e) MCP and wrist flexion/extension simultaneously, random. During rhythm trials, the subjects were instructed to conduct cyclical movements in either direction for each DOF at a fixed frequency (1/4 Hz) [26], [27]. During random trials, the subjects were asked to conduct movements at a variable speed. 2) MCP and Wrist Joints Constrained (MWJC): as shown in Fig. 1b, the subjects were instructed to sit on a chair with the elbow at 120°and the subject's right MCP and wrist joints were fixed by the fixation device. Then, subjects performed the mirrored bilateral movement to complete the above mentioned 5 movements. The EMG signals of the subjects' right hand and the joint angles of the left hand were recorded simultaneously. Nielsen et al. employed a mirrored bilateral training strategy to estimate contralateral wrist torque by EMG of the ispi-side limb [15]. Jiang et al. employed a mirrored bilateral training strategy for simultaneous and proportional estimation of wrist kinematics in unilateral transradial amputees [32]. These studies showed that mirrored bilateral training could well solve the problem of estimating human joint kinematic parameters from contralateral EMG signals. For unilateral transradial amputees, mirrored bilateral training can be used to collect EMG signals and kinematic parameters. Prior to the experiment, the maximum voluntary contraction (MVC) of the EMG signals was recorded. The subjects maintained the MVC and performed four movements (Wrist flex - MCP flex - Wrist ext - MCP ext), each movement lasted 4 seconds, and switched to neutral posture for 1 second. During the experiment, each type of movement was performed for 20 seconds, and each movement was repeated 4 times. To avoid muscle fatigue, a rest period of 2 minutes to 3 minutes was provided between two consecutive trials. Each subject performed a total of 40 trials (5 movements × 4 trials × 2 scenarios).

(a) (b)

Fig. 1. a. MCP and Wrist Joints Unconstrained (MWJU). b. MCP and Wrist Joints Constrained (MWJC).

During the experiment, the EMG signals were recorded by the DTS sensors at 3000 Hz. Kinematic data for joint angles were recorded by the M-Hand data glove with the sampling frequency at 120 Hz. As shown in Fig. 2, the DTS sensors were attached to four muscles in sequence: 1. extensor carpi radialis, 2. extensor digitorum, 3. flexor carpi radialis, 4. flexor digitorum. The skin surface was wiped with an alcohol pad to reduce impedance before placing the electrodes. In the MWJU scenario, the right hand wore the data glove, EMG signals and joint angles of the right hand were recorded simultaneously. In the MWJC scenario, as shown in Fig. 3, the left hand wore the data glove and the right hand attached the DTS sensor. The kinematic data of the left hand and EMG signals of the right hand were collected simultaneously while the left and right hand performed mirrored bilateral movements.

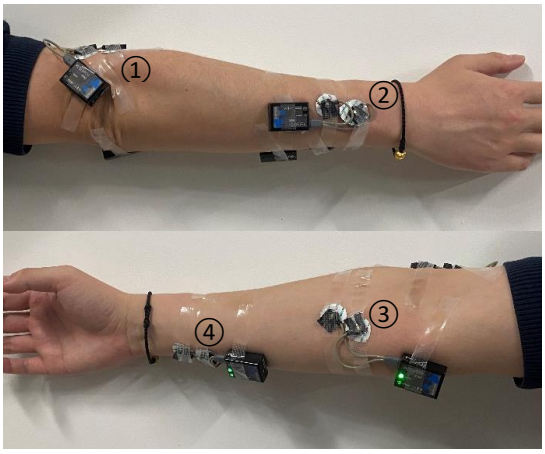

Fig. 2. EMG sensors positioning on the forearm. Four muscles: 1. extensor carpi radialis, 2. extensor digitorum, 3. flexor carpi radialis, 4. flexor digitorum

Fig. 3. Experimental set-up for the mirror bilateral training. The left hand wore the data glove and the right hand attached DTS sensor

C. Data Preprocessing

In this study, the sampling frequency of the EMG signals was 3000 Hz. The raw EMG signals were band-pass filtered (10-1000 Hz) and then full-wave rectified. The rectified signals were low-pass filtered with a 4th-order Butterworth filter at 5 Hz, and then filtered with a moving root mean square filter (window length: 500 sample points, increment: 25 sample points). Finally, the preprocessed EMG signals were normalized according to the EMG signals recorded during MVC. After the processing, the sampling frequency of EMG signals was down-sampled to 120 Hz, which ensured the sampling frequency of the EMG signals was consistent with that of the kinematic data.

D. Algorithms Modeling

A half of the experimental data was used to optimize the model parameters (5 movements × 2 trials × 2 scenarios). Then, the remaining half of the experimental data was employed to evaluate the performance of the model. Regarding the musculoskeletal model, the EMG-driven musculoskeletal model was adopted [25], [33]. The model included two degrees of freedom, MCP and wrist flexion/extension. Unlike the complex modeling of other musculoskeletal models, our musculoskeletal model only included 4 muscles. The extensor carpi radialis and flexor carpi radialis only cross the wrist joint. The extensor digitorum and flexor digitorum cross both the wrist and MCP joints. The musculoskeletal model permits independent control of wrist and MCP joint movement in both directions. Six parameters were optimized for each muscle: optimal muscle length, muscle length at a neutral position, maximum isometric force, parallel elastic element stiffness, and moment arms at the wrist flexion/extension and MCP flexion/extension. We set the moment arms to zero at joints in which a muscle does not cross anatomically. Therefore, we need to optimize 22 muscle parameters in total. To minimize the root mean square error between estimated and measured joint angles, we constrained all 22 parameters of the model within the approximate range of physiological values [28] and adopted the optimization function GlobalSearch in MATLAB to customize muscle parameters for each subject.

E. Evaluation Metrics and Methods

For all subjects, the musculoskeletal model was employed to predict MCP and wrist joint angles from EMG signals. As shown in Fig. 4, to compare the results of the two scenarios, we computed Pearson's correlation coefficient (r) and normalized root mean square error (NRMSE) between the estimated and measured angles for each joint.

$$r_{x,y} = \frac{\sum_{i=1}^{n}(x_i - \overline{x}) \cdot (y_i - \overline{y})}{\sqrt{\sum_{i=1}^{n}(x_i - \overline{x})^2 \cdot (y_i - \overline{y})^2}} \tag{1}$$

Where x_i represented the ith measured joint angles, y_i represented the ith predicted joint angels, $\bar{x}$ represented the mean value of the all measured joint angles, $\bar{y}$ represented

the mean value of the all predicted joint angles, n represented the amount of sample data.

$$NRMSE_{x,y} = \frac{\sqrt{\frac{1}{n} \cdot \sum_{i=1}^{n} (x_i - y_i)^2}}{x_{max} - x_{min}} \quad (2)$$

Where x_i represented the ith measured joint angles, y_i represented the ith predicted joint angels, x_{max} represented the maximum value of the all measured joint angles, x_{min} represented the minimum value of the all measured joint angles, n represented the amount of sample data.

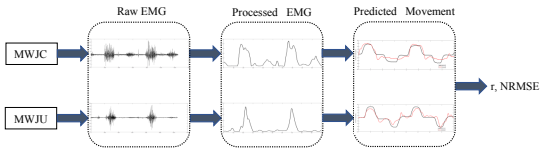

Fig. 4. The process of comparing the MWJU and MWJC.

F. Statistical Analysis

A three-way ANOVA was performed on r and NRMSE to observe the effect of variables on the results and the interaction effect between different variables. The three independent variables were joint state (MWJU and MWJC), DOF (wrist flexion/extension, MCP flexion/extension), and movement (single and simultaneously). Johnson transformation was performed on the data of r and NRMSE to ensure the data follow a normal distribution prior to the ANOVA. A full statistical model was established to observe whether had a significant interaction of three independent variables. If a significant interaction was discovered, a simple effects analysis of the levels of the interaction factor was required. If no interaction was discovered, a reduced ANOVA was performed. There was no significant interaction among the three independent variables in this experiment. One-way ANOVA was conducted with joint state, DOF, and movement as independent variables respectively to observe r and NRMSE. There were significant differences between the levels of each factor. The significance level for all tests was set to p=0.05.

III. Results

Fig. 5 shows the measured and estimated joint angles of the MCP and wrist flexion/extension during the simultaneous movements for MWJU and MWJC for the subject1. Fig. 5a shows the simultaneous wrist-MCP flexion/extension at MWJU. Fig. 5b shows the simultaneous wrist-MCP flexion/extension at MWJC. The predicted joint angles in the scenario of MWJU were much closer to the measured angles when compared to that in the scenario of the MWJC.

Fig. 6 shows the average r values across all subjects for MWJU and MWJC. For MWJU, the average r values of the wrist and MCP flexion/extension were 0.89 and 0.86 for single-DOF movements and 0.85 and 0.78 for simultaneous

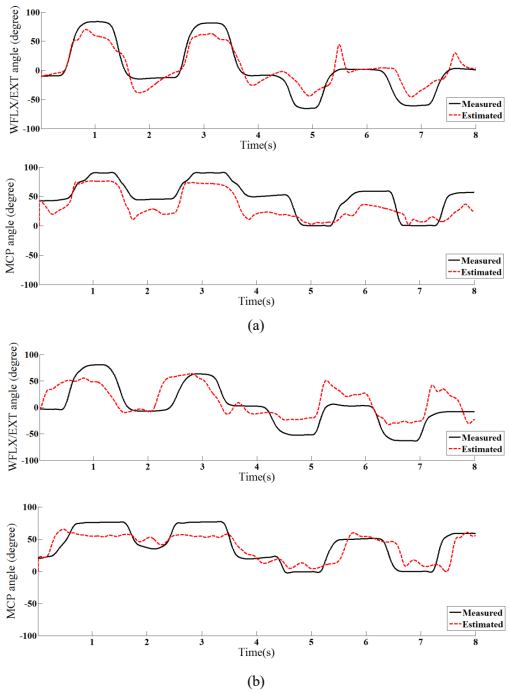

Fig. 5. (a) the simultaneous wrist-MCP flexion/extension with the MAWJU for subject Sub 1. (b) the simultaneous wrist-MCP flexion/extension with the MAWJC for subject Sub 1.

movements. For MWJC, the average r values of the wrist and MCP flexion/extension were 0.82 and 0.52 for single-DOF movements and 0.77 and 0.48 for simultaneous movements. Three-way ANOVA revealed no significant three-way or two-way interactions among joint state, DOF, and movement (joint state × DOF: p = 0.89, joint state × movement: p = 0.29, DOF × movement: p = 0.74, joint state × DOF × movement: p = 0.39). ANOVA with only main effects showed that joint state, DOF, and movement had a significant effect on r (joint state: $p < 0.001$, DOF: < 0.001, movement: p = 0.001). Compared to with the MWJU, with the MWJC, the average r values of wrist-only flexion/extension decreased by 0.07, the average r values of MCP-only flexion/extension decreased by 0.34, the average r values of simultaneous wrist flexion/extension decreased by 0.08, and the average r values of simultaneous MCP flexion/extension decreased by 0.3.

Fig. 7 shows the average NRMSE values across all subjects for MWJU and MWJC. For MWJU, the average NRMSE values of the wrist and MCP flexion/extension were 0.18 and 0.22 for single-DOF movements and 0.18 and 0.23 for simultaneous movements. For MWJC, the average NRMSE values of the wrist and MCP flexion/extension were 0.21 and 0.31 for single-DOF movements and 0.23 and 0.32 for simultaneous movements. Three-way ANOVA revealed no significant three-way or two-way interactions among joint state, DOF, and movement (joint state × DOF: p = 0.31, joint state × movement: p = 0.87, DOF × movement: p = 0.77, joint state × DOF × movement: p = 0.54). ANOVA with only main effects showed that joint state, DOF, and movement had a

significant effect on r (joint state: $p < 0.001$, DOF: < 0.001, movement: $p < 0.01$). Compared to with the MWJU, with the MWJC, the average NRMSE values were higher in all conditions.

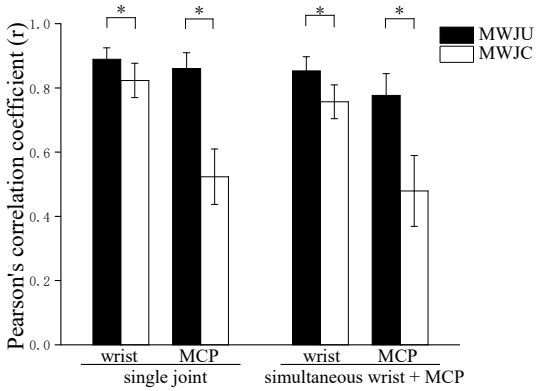

Fig. 6. Pearson's correlation coefficient (r) between measured and predicted joint angles during single-joint and simultaneous multi-joint (MCP and wrist) movements.

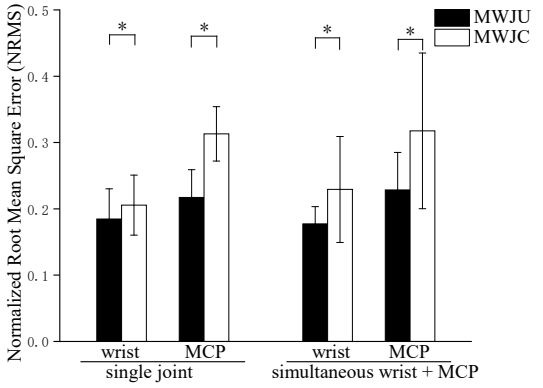

Fig. 7. NRMSE between measured and predicted joint angles during single-joint and simultaneous multi-joint (MCP and wrist) movements.

IV. Discussion

In this study, we investigated whether the movement of the MCP and wrist joints affected continuous movement decoding. We compared the continuous movement decoding performance of MWJU and MWJC. In the MWJU scenario, subjects performed the 5 types of movements naturally. In the MWJC scenario, the wrist and MCP joints of the subjects were constrained by our device. In this scenario, the subject was similar to an amputee without the hand joints, but such constraint didn't fully represent the reality of amputees. The subject's hand and the support of the device still have interaction. The 5 different types of movements adopted in this experiment were based on our previous studies [26], [27]. We considered these 5 types of movements to be representative of MCP and wrist movements in daily life. The ¼ Hz frequency was chosen because MCP and wrist movements at this speed can be considered moderate in daily life [26]. We quantified the continuous movement decoding performance by calculating the r value and NRMSE value between the predicted and measured joint angles. The experimental results indicated that compared with MWJU, MWJC had a significant effect on continuous movement decoding.

Fig. 5 shows the predicted and the measured joint angles in the simultaneous wrist-MCP flexion/extension trials for subject Sub 1. MWJU achieved a better prediction performance in terms of waveform and amplitude. The average r values of MWJU at wrist and MCP were 0.89 and 0.86, and the average r values of MWJC at wrist and MCP were 0.82 and 0.52. The result of the estimation performance (r and NRMSE) with MWJU was significantly better than that with MWJC. Compared to MWJC, the better performance and higher reliability of MWJU in different movements might be caused by the following reasons: the movement of the MCP and wrist joints induced the displacement of the subcutaneous muscle, so that the EMG electrode on the skin surface was displaced and the obtained EMG signals change. The EMG signals generated by joint movement collected with the MWJU contained more information for continuous movement decoding. Therefore, the performance of continuous movement decoding was much better. In our previous studies, we demonstrated that the joint movement caused the displacement of the subcutaneous muscle relative to the electrodes on the skin surface by ultrasound [13]. The results also supported the above explanations.

Compared to MWJU, we found that the r values of the wrist joint decreased by 0.07 for MWJC, while the r values of MCP decreased by 0.34 for MWJC. As shown in Fig. 8, we compared the muscle activation of MCP flexion/extension in the two scenarios. The red box indicated the phenomenon of muscle co-contraction. The muscle activation of ECR and FCR were 0.16 and 0.09 for MWJU. The muscle activation of ECR and FCR were 0.26 and 0.22 for MWJC. We considered that the MCP flexion/extension might induce stronger co-contraction of the muscles while the joints were constrained. Meanwhile, it could be generated by the reason that the subject was exploiting the forces produced in the interaction between his hand and the support to generate the desired movement. This phenomenon may induce that the extensor carpi radialis and flexor carpi radialis were involved when subjects performed the MCP flexion/extension, resulting in poor prediction performance of joint angles.

There are many reasons for the poor performance of continuous movement decoding in amputees. Such as muscle loss/shortening and reattachment, due to surgery, impact the contraction level of the muscles in the stump compromising the efficiency of the decoding. Our study can only indicate that the absence of joint movement is one of the factors causing the poor performance of continuous movement decoding in amputees. We hoped that this study could provide a new consideration for the poor performance of continuous movement decoding in amputees. There were several limitations in this study. The selected muscles flexor digitorum and extensor digitorum are biarticular muscle that

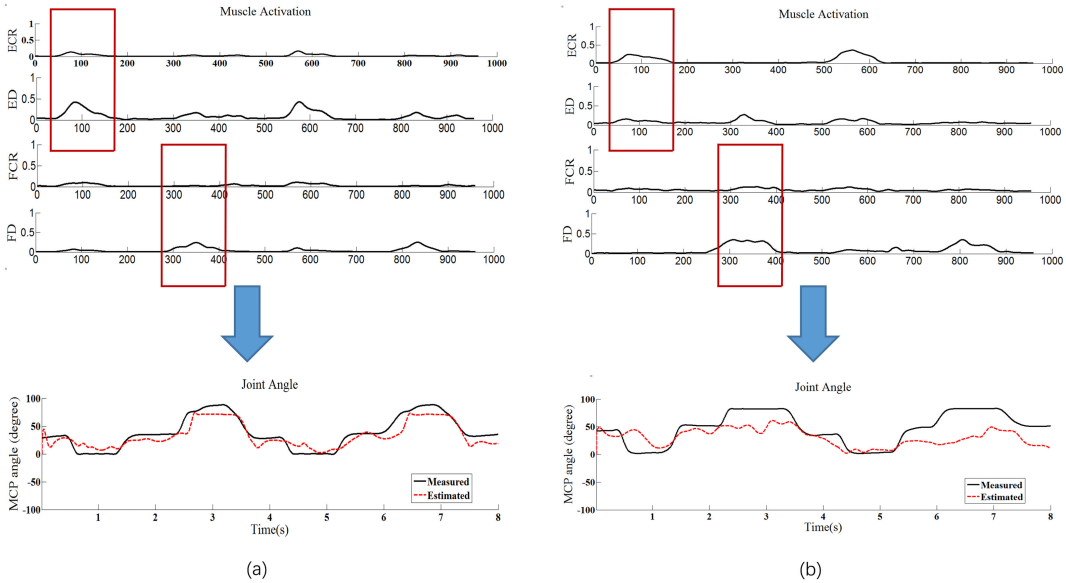

Fig. 8. (a) Muscle Activation and Joint Angle of MCP flexion/extension with the MAWJU for subject Sub 1. (b) Muscle Activation and Joint Angle of MCP flexion/extension with the MAWJC for subject Sub 1. The red box indicated the phenomenon of muscles co-contraction.

works synergically with flexor carpi radialis and extensor carpi radialis so to guarantee independent control of the wrist and MCP flexion-extension. In the moment one of the two joints is constrained the subject does not need to apply the same control strategy to lock one of the two joints because external forces are doing the job for him. Even if we constrained the subjects' wrist and MCP joints, the muscle contractions were inherently different. The change of the joint angles produces different muscle elongation and torque arms. The muscle contraction of the constrained modality in our experiments was not fully representative of the actual muscle contraction in amputees. In the future, we will recruit and test amputee subjects for further research. Then we will compare the performance of continuous movement decoding between the affected and unaffected sides of unilateral transradial amputee patients. The current study was an offline analysis. We will compare the real-time EMG continuous decoding performance with MWJU and MWJC in our future work. There are over 40 muscles that may contribute to wrist and hand movement, but only four muscles were included in the musculoskeletal model. The simplification of hand structure may lead to kinematic prediction error. We will continue to optimize and improve our musculoskeletal model in the future.

V. Conclusion

In this study, we investigated the effect of MCP and wrist joints movement on continuous movement decoding. The experimental results indicated that compared to with the MWJU, with the MWJC, the average r values of wrist-only flexion/extension decreased by 0.07, the average r values of MCP-only flexion/extension decreased by 0.34, the average r values of simultaneous wrist flexion/extension decreased by 0.08, and the average r values of simultaneous MCP flexion/extension decreased by 0.3. The results implied that the MWJC made continuous movement decoding worse, and the lack of joint movements in amputees compared to able-bodied subjects might be one of the factors that contributed to the poor performance of continuous movement decoding.

Acknowledgment

The authors thank all participants who took part in the study.

References

[1] B. Hudgins, P. Parker, and R. N. Scott, "A new strategy for multifunction myoelectric control," *IEEE transactions on biomedical engineering*, vol. 40, no. 1, pp. 82–94, 1993.

[2] D. Xiong, D. Zhang, X. Zhao, and Y. Zhao, "Deep learning for emg-based human-machine interaction: a review," *IEEE/CAA Journal of Automatica Sinica*, vol. 8, no. 3, pp. 512–533, 2021.

[3] K. Li, J. Zhang, L. Wang, M. Zhang, J. Li, and S. Bao, "A review of the key technologies for semg-based human-robot interaction systems," *Biomedical Signal Processing and Control*, vol. 62, p. 102074, 2020.

[4] Q. Zhang, K. Kim, and N. Sharma, "Prediction of ankle dorsiflexion moment by combined ultrasound sonography and electromyography," *IEEE Transactions on Neural Systems and Rehabilitation Engineering*, vol. 28, no. 1, pp. 318–327, 2019.

[5] L. Pan, D. Zhang, X. Sheng, and X. Zhu, "Improving myoelectric control for amputees through transcranial direct current stimulation," *IEEE Transactions on Biomedical Engineering*, vol. 62, no. 8, pp. 1927–1936, 2015.

[6] A. Dellacasa Bellingegni, E. Gruppioni, G. Colazzo, A. Davalli, R. Sacchetti, E. Guglielmelli, and L. Zollo, "Nlr, mlp, svm, and lda: a comparative analysis on emg data from people with trans-radial amputation," *Journal of neuroengineering and rehabilitation*, vol. 14, no. 1, pp. 1–16, 2017.

[7] M. Atzori, A. Gijsberts, C. Castellini, B. Caputo, A.-G. Mittaz Hager, S. Elsig, G. Giatsidis, F. Bassetto, and H. Müller, "Clinical parameter effect on the capability to control myoelectric robotic prosthetic hands," *Journal of rehabilitation research and development*, vol. 53, no. 3, pp. 345–358, 2016.

[8] N. Jiang, S. Muceli, B. Graimann, and D. Farina, "Effect of arm position on the prediction of kinematics from emg in amputees," *Medical & biological engineering & computing*, vol. 51, no. 1, pp. 143–151, 2013.

[9] Z. Taghizadeh, S. Rashidi, and A. Shalbaf, "Finger movements classification based on fractional fourier transform coefficients extracted from surface emg signals," *Biomedical Signal Processing and Control*, vol. 68, p. 102573, 2021.

[10] C. Cipriani, C. Antfolk, M. Controzzi, G. Lundborg, B. Rosén, M. C. Carrozza, and F. Sebelius, "Online myoelectric control of a dexterous hand prosthesis by transradial amputees," *IEEE Transactions on Neural Systems and Rehabilitation Engineering*, vol. 19, no. 3, pp. 260–270, 2011.

[11] M. A. Powell, R. R. Kaliki, and N. V. Thakor, "User training for pattern recognition-based myoelectric prostheses: Improving phantom limb movement consistency and distinguishability," *IEEE Transactions on Neural Systems and Rehabilitation Engineering*, vol. 22, no. 3, pp. 522–532, 2013.

[12] A. Waris, I. K. Niazi, M. Jamil, O. Gilani, K. Englehart, W. Jensen, M. Shafique, and E. N. Kamavuako, "The effect of time on emg classification of hand motions in able-bodied and transradial amputees," *Journal of Electromyography and Kinesiology*, vol. 40, pp. 72–80, 2018.

[13] L. Pan, K. Liu, and J. Li, "Effect of subcutaneous muscle displacement on surface electromyography," *IEEE transactions on neural systems and rehabilitation engineering*, major revision.

[14] L. Pan, K. Liu, K. Zhu, and J. Li, "Comparing emg pattern recognition with and without hand and wrist movements," *Journal of Bionic Engineering*, pp. 1–9, 2022.

[15] J. L. Nielsen, S. Holmgaard, N. Jiang, K. B. Englehart, D. Farina, and P. A. Parker, "Simultaneous and proportional force estimation for multifunction myoelectric prostheses using mirrored bilateral training," *IEEE Transactions on Biomedical Engineering*, vol. 58, no. 3, pp. 681–688, 2010.

[16] J. M. Hahne, F. Biessmann, N. Jiang, H. Rehbaum, D. Farina, F. C. Meinecke, K.-R. Müller, and L. C. Parra, "Linear and nonlinear regression techniques for simultaneous and proportional myoelectric control," *IEEE Transactions on Neural Systems and Rehabilitation Engineering*, vol. 22, no. 2, pp. 269–279, 2014.

[17] J. Hahne, H. Rehbaum, F. Biessmann, F. C. Meinecke, K.-R. Müller, N. Jiang, D. Farina, and L. C. Parra, "Simultaneous and proportional control of 2d wrist movements with myoelectric signals," in *2012 IEEE international workshop on machine learning for signal processing*. IEEE, 2012, pp. 1–6.

[18] Y. Koike and M. Kawato, "Estimation of dynamic joint torques and trajectory formation from surface electromyography signals using a neural network model," *Biological cybernetics*, vol. 73, no. 4, pp. 291–300, 1995.

[19] J. G. Ngeo, T. Tamei, and T. Shibata, "Continuous and simultaneous estimation of finger kinematics using inputs from an emg-to-muscle activation model," *Journal of neuroengineering and rehabilitation*, vol. 11, no. 1, pp. 1–14, 2014.

[20] Y. Chen, X. Zhao, and J. Han, "Hierarchical projection regression for online estimation of elbow joint angle using emg signals," *Neural Computing and Applications*, vol. 23, no. 3, pp. 1129–1138, 2013.

[21] D. Di Domenico, A. Marinelli, N. Boccardo, M. Semprini, L. Lombardi, M. Canepa, S. Stedman, A. D. Bellingegni, M. Chiappalone, E. Gruppioni *et al.*, "Hannes prosthesis control based on regression machine learning algorithms," in *2021 IEEE/RSJ International Conference on Intelligent Robots and Systems (IROS)*. IEEE, 2020, pp. 5997–6002.

[22] A. Ameri, E. N. Kamavuako, E. J. Scheme, K. B. Englehart, and P. A. Parker, "Support vector regression for improved real-time, simultaneous myoelectric control," *IEEE Transactions on Neural Systems and Rehabilitation Engineering*, vol. 22, no. 6, pp. 1198–1209, 2014.

[23] P. K. Artemiadis and K. J. Kyriakopoulos, "A switching regime model for the emg-based control of a robot arm," *IEEE Transactions on Systems, Man, and Cybernetics, Part B (Cybernetics)*, vol. 41, no. 1, pp. 53–63, 2010.

[24] L. Pan, D. Zhang, J. Liu, X. Sheng, and X. Zhu, "Continuous estimation of finger joint angles under different static wrist motions from surface emg signals," *Biomedical Signal Processing and Control*, vol. 14, pp. 265–271, 2014.

[25] L. Pan, D. L. Crouch, and H. Huang, "Myoelectric control based on a generic musculoskeletal model: Toward a multi-user neural-machine interface," *IEEE Transactions on Neural Systems and Rehabilitation Engineering*, vol. 26, no. 7, pp. 1435–1442, 2018.

[26] D. L. Crouch and H. Huang, "Lumped-parameter electromyogram-driven musculoskeletal hand model: A potential platform for real-time prosthesis control," *Journal of biomechanics*, vol. 49, no. 16, pp. 3901–3907, 2016.

[27] L. Pan, D. L. Crouch, and H. Huang, "Comparing emg-based human-machine interfaces for estimating continuous, coordinated movements," *IEEE transactions on neural systems and rehabilitation engineering*, vol. 27, no. 10, pp. 2145–2154, 2019.

[28] D. L. Crouch and H. H. Huang, "Musculoskeletal model-based control interface mimics physiologic hand dynamics during path tracing task," *Journal of neural engineering*, vol. 14, no. 3, p. 036008, 2017.

[29] D. Blana, J. G. Hincapie, E. K. Chadwick, and R. F. Kirsch, "A musculoskeletal model of the upper extremity for use in the development of neuroprosthetic systems," *Journal of biomechanics*, vol. 41, no. 8, pp. 1714–1721, 2008.

[30] M. Sartori, G. Durandau, S. Došen, and D. Farina, "Robust simultaneous myoelectric control of multiple degrees of freedom in wrist-hand prostheses by real-time neuromusculoskeletal modeling," *Journal of neural engineering*, vol. 15, no. 6, p. 066026, 2018.

[31] G. Durandau, D. Farina, and M. Sartori, "Robust real-time musculoskeletal modeling driven by electromyograms," *IEEE transactions on biomedical engineering*, vol. 65, no. 3, pp. 556–564, 2017.

[32] N. Jiang, J. L. Vest-Nielsen, S. Muceli, and D. Farina, "Emg-based simultaneous and proportional estimation of wrist/hand kinematics in uni-lateral trans-radial amputees," *Journal of neuroengineering and rehabilitation*, vol. 9, no. 1, pp. 1–11, 2012.

[33] D. L. Crouch, L. Pan, W. Filer, J. W. Stallings, and H. Huang, "Comparing surface and intramuscular electromyography for simultaneous and proportional control based on a musculoskeletal model: A pilot study," *IEEE Transactions on Neural Systems and Rehabilitation Engineering*, vol. 26, no. 9, pp. 1735–1744, 2018.